Journal of Biomedical Optics

SPIEDigitalLibrary.org/jbo

Confocal Raman data analysis enables identifying apoptosis of MCF-7 cells caused by anticancer drug paclitaxel

Hamideh Salehi
Elodie Middendorp
Ivan Panayotov
Pierre-Yves Collart Dutilleul
Attila-Gergely Vegh
Sathish Ramakrishnan
Csilla Gergely
Frederic Cuisinier

SPIE

Confocal Raman data analysis enables identifying apoptosis of MCF-7 cells caused by anticancer drug paclitaxel

Hamideh Salehi,[a] Elodie Middendorp,[a] Ivan Panayotov,[a] Pierre-Yves Collart Dutilleul,[a] Attila-Gergely Vegh,[a,b] Sathish Ramakrishnan,[c,d] Csilla Gergely,[c,d] and Frederic Cuisinier[a]
[a]Université Montpellier 1, Laboratoire Biologie-Santé Nanosciences, EA 4203, UFR Odontologie, 34193 Montpellier, France
[b]Institute of Biophysics, Hungarian Academy of Sciences, Biological Research Centre, 6726 Szeged, Hungary
[c]Université Montpellier 2, Laboratoire Charles Coulomb UMR 5221, 34095 Montpellier, France
[d]CNRS, Laboratoire Charles Coulomb UMR 5221, 34095 Montpellier, France

Abstract. Confocal Raman microscopy is a noninvasive, label-free imaging technique used to study apoptosis of live MCF-7 cells. The images are based on Raman spectra of cells components, and their apoptosis is monitored through diffusion of cytochrome *c* in cytoplasm. K-mean clustering is used to identify mitochondria in cells, and correlation analysis provides the cytochrome *c* distribution inside the cells. Our results demonstrate that incubation of cells for 3 h with 10 μM of paclitaxel does not induce apoptosis in MCF-7 cells. On the contrary, incubation for 30 min at a higher concentration (100 μM) of paclitaxel induces gradual release of the cytochrome *c* into the cytoplasm, indicating cell apoptosis via a caspase independent pathway. [DOI: 10.1117/1.JBO.18.5.056010]

Keywords: apoptosis; Raman microscopy; paclitaxel; K-mean cluster; correlation coefficient; living cell.

Paper 130019PRR received Jan. 14, 2013; revised manuscript received Mar. 31, 2013; accepted for publication Apr. 12, 2013; published online May 9, 2013; corrected May 29, 2013.

1 Introduction

A common method for monitoring the distribution of drugs in fixed and live cells is fluorescent labeling.[1] However, low contrast and photobleaching often impede fluorescence imaging, and the introduction of fluorescent labels may change the molecule's biochemical properties. Confocal Raman microscopy is a powerful and unique tool for cell imaging and protein conformation imaging.[2,3] The Raman spectra of cells contain the fingerprints of all molecules present, so they are very complex. Individual cells' Raman spectra [4,5] and the localization of intracellular nanoparticles[6–8] have been reported previously. High spatial resolution and a unique compositional sensitivity are the main advantages of confocal Raman microscopy over other spectroscopic methods.[1] A drug's Raman signature enables its detection in the cell without the need for labeling. A cell's biochemical composition in the laser spot volume can be recorded as its Raman spectra. Moreover, multivariate methods of analysis can be applied to enhance the relatively small spectral contrast between cellular components.[9]

Paclitaxel has been greatly used in medicine[10–12] and as a pro-apoptotic drug[13–16] in cell biology research. Paclitaxel ($C_{47}H_{51}NO_{14}$, molecular weight[14] 835 Da) is categorized as a microtubule-stabilizing agent.[14] By binding to a second site, the paclitaxel molecule can form a groove between α-tubulin and β-tubulin monomers.[17]

Apoptosis (programmed cell death) is a cellular self-destruction mechanism that is essential for a variety of biological events, such as developmental sculpturing, tissue homeostasis, and removal of unwanted cells. Mitochondria play a crucial role in regulating cell death.[1,18] The proteases, known as caspases, are activated through extrinsic and/or intrinsic pathways. The extrinsic pathway is activated by cell surface death receptors, while the intrinsic pathway is initiated by the formation of the cytosolic apoptosome composed of Apaf-1, procaspase 9, and the cytochrome *c* released from mitochondria.[19] We used confocal Raman microscopy to monitor the paclitaxel, mitochondria, and cytochrome *c* within cells. The presence of cytochrome *c* outside of mitochondria would indicate the start of apoptosis via a mitochondrial apoptosis pathway independent of the caspase 8/t-Bid pathway.[20]

2 Materials and Methods

2.1 *Cell Culture*

The MCF-7 cell line, first derived from a metastatic breast cancer patient in 1970, was the first cancer cell line capable of living longer than a few months and has become a standard model in cancer research laboratories.[21] MCF-7 cells were grown in 75-cm^2 culture flasks (VWR, Strasbourg, France) in a medium containing 7 mL of Dulbecco's Modified Eagle's Medium (DMEM; Thermo Fisher, Strasbourg, France), 20% FBS, and 1% antibiotics (Streptomycin 100 μg ml^{-1} penicillin, 100 U ml^{-1}) at 37°C and 5% CO_2. Cells were cultivated on to polished calcium fluoride (CaF_2) substrates (Crystran Ltd., Dorset, UK). After 24 h, the cells adhered on the CaF_2 substrate. Cells were incubated for 3 h in a solution of DMEM containing paclitaxel and rinsed with PBS before being transferred under the confocal Raman microscope.

Address all correspondence to: Hamideh Salehi, Université Montpellier 1, Laboratoire Biologie-Santé Nanosciences, EA 4203, UFR Odontologie, 34193 Montpellier, France. Tel: +33607880499; Fax: +33467107431; E-mail: s_hamideh@yahoo.com

0091-3286/2013/$25.00

2.2 *Raman Data Acquisition*

Raman spectra were collected using a Witec Confocal Raman Microscope System alpha 300R (Witec Inc., Ulm, Germany). Excitation in the confocal Raman microscopy is assured by a frequency doubled Nd:YAG laser (Newport, Evry, France) at a wavelength of 532 nm. The incident laser beam was focused on to the sample through a 60× NIKON water immersion objective with a numerical aperture of 1.0 and a working distance of 2.8 mm (Nikon, Tokyo, Japan). Then Raman backscattered radiation mixed with Rayleigh scattered light was passed through an edge filter to block the Rayleigh scattering. The acquisition time of a single spectrum was set to 0.5 s. A piezoelectric table was used to record 150 × 150 points per image, leading to a total of 22,500 spectra for one image, each spectrum corresponding to a spatial unit defined as a voxel. Data acquisition was performed using Image Plus software from Witec.

2.3 *Data Analysis*

Data analysis was based on three methods. The first method provides integrated Raman intensities in specific regions, in particular the CH stretching mode. Data processing was performed using Image Plus software from Witec. Each image regarding these integrated intensities could provide a map of the region. Using a lookup table, bright yellow hues indicated the highest intensities, while orange hues indicated the lowest integrated intensities of the chosen region.

The second method is K-mean cluster analysis (KMCA). K-mean clustering partitions data into k mutually exclusive clusters. It treats each observation in the data set as an object having a location in space. It finds a partition in which objects within each cluster are as close to each other as possible and as far from objects in other clusters as possible. KMCA was realized using the Witec Project Plus (Ulm, Germany) software.

As a third analysis method, the spectral correlation matrix was calculated[9] to find the most similar spectrum to the reference spectrum of paclitaxel. To quantify the similarity, as a distance, the Pearson's correlation coefficient was calculated for each pair of spectra, given by

$$r = \frac{\Sigma_{i=1}^{N}((x_i - X)(y_i - Y))}{\sqrt{\Sigma_{i=1}^{N}(x_i - X)^2 \Sigma_{i=1}^{N}(y_i - Y)^2}}, \quad (1)$$

where N is the number of points within the spectrum, x_i and y_i are the individual points, and X and Y are the mean value of each spectrum. The value of r can vary between −1 and 1, and thus it

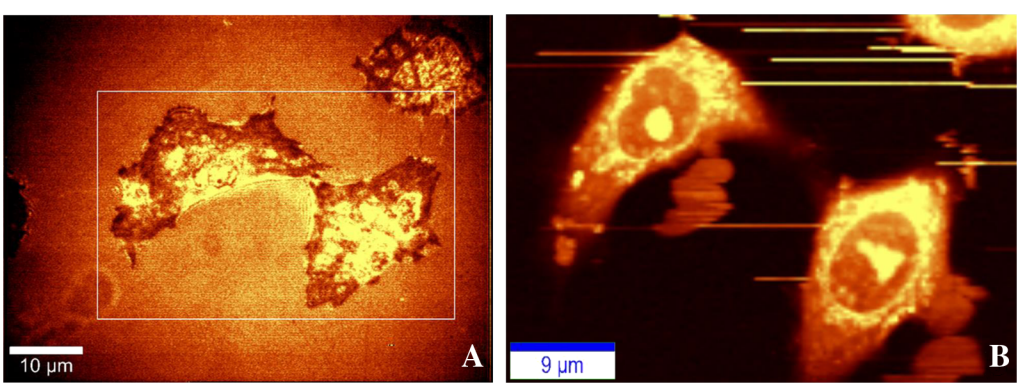

Fig. 1 (a) Bright-field microscopic image of a MCF-7 cell in buffer solution, 60× objective. (b) Integrated Raman intensities in the region of 2800 to 3000 cm^{-1} of the cell, collected at a dwell time of 0.5 s/point and a point spacing of around 300 nm. Bright yellow and dark hues indicate the highest and lowest integrated CH stretching intensities, respectively.

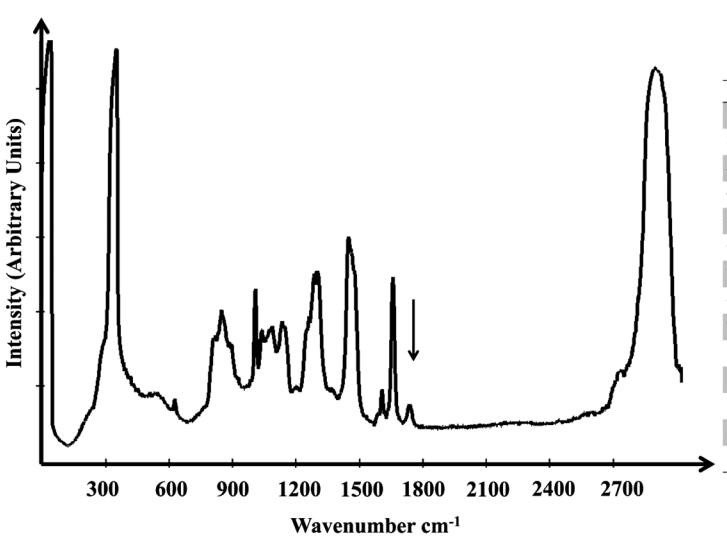

	Raman peak cm^{-1}	Assignment
1	325	C-H out of plane / C-C=O deformation
2	850	
3	887	C-H in plane deformation
4	1006	
5	1054	C-O stretching
6	1088	
7	1135	
8	1281	C-N stretching
9	1298	
10	1460	(1428) CH3 deformation
11	1609	C-C stretching
12	1654	
13	1738	C=O stretching
14	2887	CH3 / C-H stretching

Fig. 2 Predominant bands in the Raman spectra of a clinical paclitaxel solution from Teva Ind. and the assignment of relevant peaks.

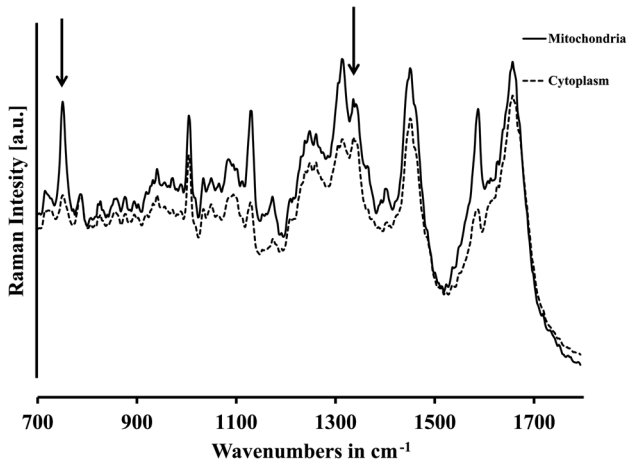

Fig. 3 Predominant bands in the Raman spectra of (solid line) cytoplasm and (dashed line) mitochondria in cell.

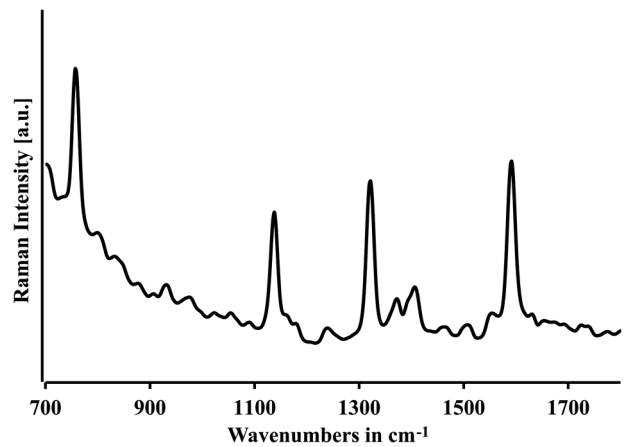

Fig. 4 Predominant bands in the Raman spectra of cytochrome c.

can be expressed as a percentage ranging from −100 (no correlation) to 100% (the perfect match). From these values, a pseudo color map can be constructed reflecting the quantified similarities. All correlation calculations were performed with a homemade code written in MatLab (Math Works Inc., Natick, Massachusetts).

2.4 *Paclitaxel*

In our experiments, paclitaxel (Taxol, Teva Pharmaceutical Ind., Tel Aviv, Israel) was added to a cell culture medium in two concentrations: 9.7 $\mu g\,ml^{-1}$ which is equivalent to the clinically used amount of paclitaxel, and a higher concentration of 100 μM. Cells were incubated for 3 h in the low concentration of paclitaxel and for 30 min in the high concentration.

2.5 *Cytochrome c*

Cytochrome *c* was bought from Sigma-Aldrich (St. Louis, Missouri). The Raman spectrum of cytochrome *c* solution in a reduced state using ascorbic acid was acquired as a reference spectrum.

3 Results

Figure 1 illustrates the data acquisition and analysis used for the intracellular detection of paclitaxel. The low contrast in the bright field image is due to the absence of staining of MCF-7 living cells in PBS solution, as shown in Fig. 1(a). The total integrated Raman intensities of the CH stretching mode in the domain of 2800 to 3000 cm^{-1} provided an image representing the quantity of proteins, as shown in Fig. 1(b). Bright yellow hues correspond to high intensities of CH stretching band inside the cell, while dark hues indicate the lowest integrated intensities of the CH stretching band belonging to PBS. This image is in good correlation with the bright field optical image of the MCF-7 cells.

The Raman spectrum of the paclitaxel solution prepared from taxol was recorded, and the results are shown in Fig. 2. The assignment of relevant peaks is gathered in the table.

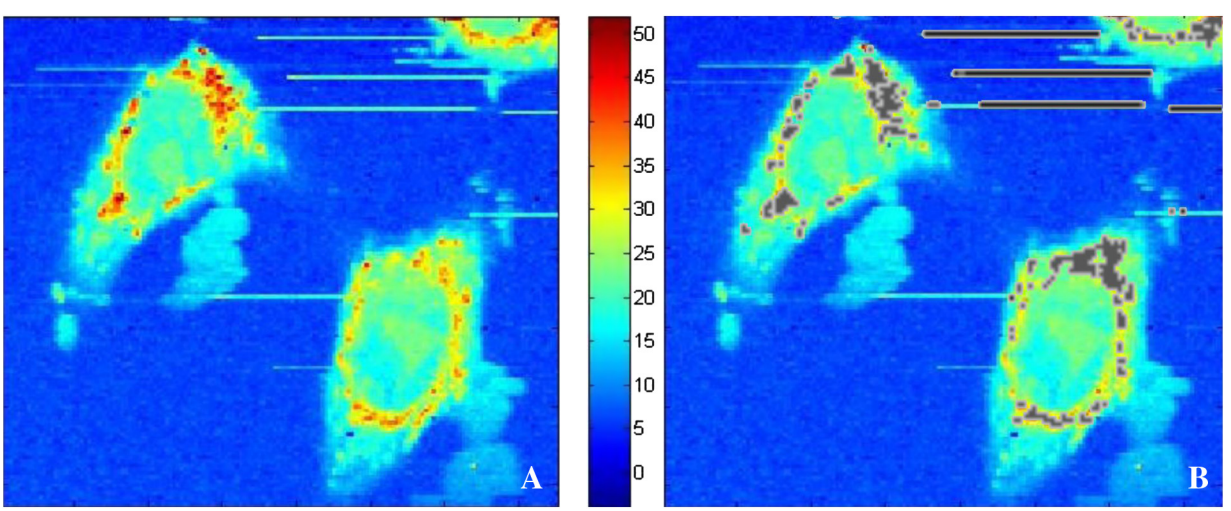

Fig. 5 (a) Correlation map and correlation coefficient between the whole cell image spectra (treated cells for 3 h with 10-μM paclitaxel from Fig. 1) and that of cytochrome *c* taken as a reference (spectrum in Fig. 4). The best correlation is obtained for the red spots: the region with more than 50% correlation between the reference spectrum of the cytochrome *c* and their spectra in the cells. The region with no correlation to cytochrome *c* is due to the PBS buffer (blue region). (b) Mitochondria cluster (gray) was overlapped with the correlation map of cytochrome *c*. All the positions corresponding to cytochrome *c* are covered. The differences between (a) and (b) indicate localization of cytochrome *c* inside mitochondria.

The Raman vibrations obtained for the paclitaxel used in our research are very similar to the spectra previously reported for functional derivatives of paclitaxel.[6]

The detailed average spectrum of a cell's cytoplasm and mitochondria calculated by KMCA are shown in Fig. 3. The number of spectra contributing to the average spectra of each cluster is on the order of thousands. Consequently, the observed signal-to-noise ratio for an average spectrum is very good. The two arrows indicate specific Raman bands of mitochondria. Because KMCA enabled us to separate the mitochondria cluster, the next step was to detect cytochrome *c* in cells.

cytochrome *c* acts as a trigger of caspase cascade activation, and its release from mitochondria is a sign of apoptosis. cytochrome *c* solution in a reduced state obtained using ascorbic

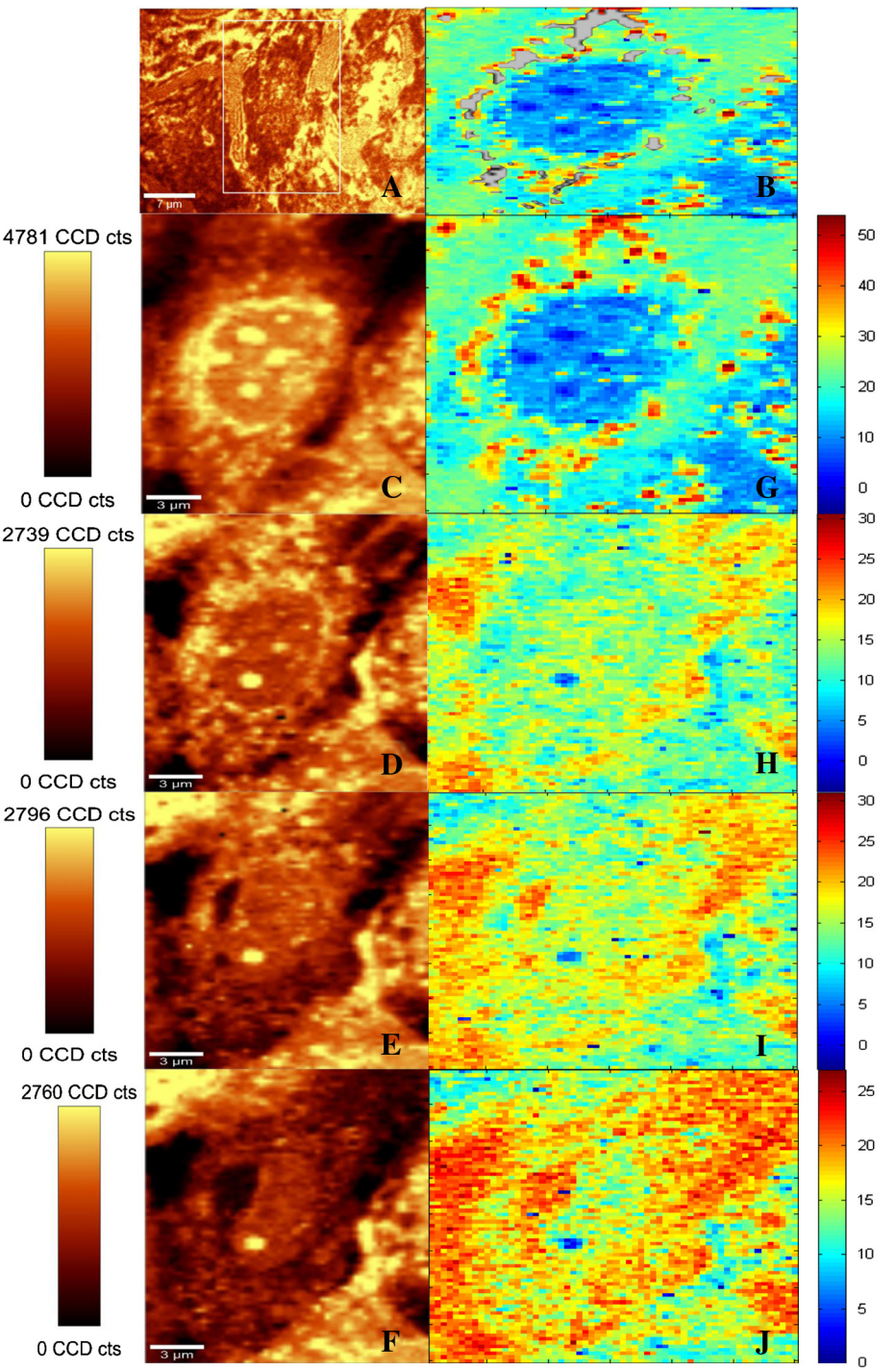

Fig. 6 (a) Bright-field microscopic image of a MCF-7 cell in buffer solution, 60× objective. (b) Overlap of the mitochondria cluster (gray) on the correlation map of cytochrome *c*. (c–f) Integrated Raman intensities in the region of 2800 to 3000 cm^{-1} of the cells shown in (a). Image (c) was collected after 30 min of contact with 100-μM paclitaxel, at a total dwell time of 60 min per image. Bright yellow and dark hues indicate the highest and lowest integrated CH stretching intensities, respectively. The images in the series (c–f) were collected sequentially with the same accumulation times. (g–j) Correlation map and the correlation coefficient between the whole cell image spectra [cells from (c–f)] and that of cytochrome *c* taken as a reference (spectrum in Fig. 4). The best correlation is indicated by the red spots.

acid was measured as a reference spectrum for the correlation coefficient map.[22,23] The Raman spectrum of the reduced cytochrome *c* is presented in Fig. 4.

As a final step in the eventual detection of apoptosis in cells, we traced cytochrome *c* within the cells. Figure 5 illustrates the correlation coefficient map of cytochrome *c* obtained by comparison of the reference spectrum of cytochrome *c* and the whole MCF-7 cell image spectra after 3 h of treatment with 10-μM paclitaxel.

In Fig. 5(a), red pixels belong to the most correlated spectra to the reference spectrum of cytochrome *c* (correlation coefficient up to 50%). As discussed before with Fig. 3, KMCA enables us to position the mitochondria in cells. Mitochondria clusters in the cell are plotted in gray in Fig. 5(b). When we superposed these clusters on the cytochrome *c* correlation map, we found that the mitochondria cluster covers all the cytochrome *c* positions in the cell. Comparing Fig. 5(a) and 5(b) clearly indicates that cytochrome *c* is localized inside the mitochondria of the MCF-7 cells.

Further, we increased the paclitaxel concentration to 100 μM, and its effect on MCF-7 cells after 30 min of incubation was monitored. Figure 6 illustrates the data acquisition and analysis used for intracellular detection of cytochrome c. Figure 6(a) is a bright field image of MCF-7 living cells in PBS solution. The mitochondria cluster overlapping the correlation map of cytochrome *c* is shown in Fig. 6(b). The gray cluster of mitochondria covers most of cytochrome *c* (red spot). Few red spots are outside the mitochondria cluster, which presents the start of releasing cytochrome *c*. The total integrated Raman intensities of the CH stretching mode in the domain of 2,800 to 3,000 cm^{-1} is provided in Fig. 6(c)–6(f). The image shown in Fig. 6(c) was collected after 30 min of contact with the 100-μM paclitaxel. Then paclitaxel was rinsed with PBS, and a series of Raman images, shown in Fig. 6(c)–6(f), were collected on the same cells at a total dwell time of 60 min per image. Bright yellow hues indicate the highest integrated CH stretching intensity, and the dark hues indicate the lowest integrated CH stretching intensity. The correlation maps of these series were created as described before, and each image spectrum was compared to the reference spectrum of cytochrome *c* (Fig. 4). A map shown in Fig. 6(g)–6(j) presents the most correlated points to reference. The best correlation is indicated by the red spots. A comparison of Fig. 6(g) with 6(j) demonstrates the gradual release of cytochrome *c* from mitochondria.

4 Discussion

A key issue in presenting evidence of cell apoptosis is detecting the release of cytochrome *c* by mitochondria. Previous methods to monitor modifications in cell organelles have involved extensive sample preparation for electron microscopy or staining mitochondria using fluorescent dyes, but these are rather invasive methods that might disturb the normal cell cycle. Confocal Raman microscopy enables us to overcome these problems and provides a noninvasive method to study live cells. The spectral contrasts between cellular components are relatively small, because they are very similar in terms of Raman vibrations, but with appropriate data treatment, it is possible to reveal very small differences between the various parts of the cell.[9,24] The Raman reference spectra of mitochondria, cytoplasm, and nuclei were previously published.[1] Also, previous research has monitored mitochondrial respiration activity *in vivo* and *in vitro* by quantifying the redox states of cytochrome b and c simultaneously without using any labeling or genetic manipulation.[25] Other treatments, such as docetaxel in lower concentrations and with longer contact times with cells, have been studied.[26] In this study, we demonstrate the possibility of detecting apoptosis in cells merely by post-measurement data analysis, which is a novel method and to best of our knowledge has not been previously reported. As mentioned before, cytochrome *c* acts as a trigger of caspase cascade activation, and its release from mitochondria is a sign of apoptosis. By measuring cytochrome *c* spectrum as a reference and comparing it with all other spectra of the Raman image of the cell, we were able to obtain the correlation coefficient map of cytochrome *c*. When MCF-7 cells were in contact for 3 h with paclitaxel at a low concentration, no released cytochrome *c* was observed, but it was localized within mitochondria. When the paclitaxel concentration was increased to 100 μM, our Raman image sequences (recorded with intervals of 60 min) of treated cells showed evidence of the gradual release of cytochrome *c* into cytoplasm. The main interest of this study is that it demonstrates the ability of Raman microscopy to go beyond detection of intracellular drugs. The effect of paclitaxel on MCF-7 cells was successfully imaged by monitoring cytochrome *c* release in cytoplasm for several hours.

5 Conclusion

This study demonstrates the ability of confocal Raman microscopy to detect apoptosis mediated by cytochrome *c* release from mitochondria. A comparison between localization of clusters of mitochondria and those of cytochrome *c* within the MCF-7 cells provides evidence that cytochrome *c* is inside the mitochondria after 3 h of incubation with paclitaxel at 9.7 μM (a clinically used concentration). A higher concentration (100 μM) of paclitaxel triggers the release of cytochrome *c* into the cytoplasm. Confocal Raman microscopy is a powerful technique for label-free and noninvasive detection of drugs and monitoring their diffusion within cells. Moreover, our novel post-measurement data analysis methods enabled the identification of the drug-induced cell apoptosis as one occurring via a mitochondria pathway.

References

1. C. Matthäus et al., "Label-free detection of mitochondrial distribution in cells by nonresonant Raman microspectroscopy," *Biophys. J.* **93**(2), 668–673 (2007).
2. M. M. Mariani, P. J. Day, and V. Deckert, "Applications of modern micro-Raman spectroscopy for cell analyses," *Integr. Biol. (Camb).* **2**(2–3), 94–101 (2010).
3. K. E. Shafer-Peltier et al., "Model-based biological Raman spectral imaging," *J. Cell. Biochem. Suppl.* **87**(Suppl. 39), 125–137 (2002).
4. C. Krafft, B. Dietzek, and J. Popp, "Raman and CARS microspectroscopy of cells and tissues," *Analyst* **134**(6), 1046–1057 (2009).
5. K. Hartmann et al., "A study of Docetaxel-induced effects in MCF-7 cells by means of Raman microspectroscopy," *Anal. Bioanal. Chem.* **403**(3), 745–753 (2012).
6. J. Dorney et al., "Identifying and localizing intracellular nanoparticles using Raman spectroscopy," *Analyst* **137**(5), 1111–1119 (2012).
7. T. Chernenko et al., "Label-free Raman spectral imaging of intracellular delivery and degradation of polymeric nanoparticle systems," *ACS Nano* **3**(11), 3552–3559 (2009).
8. L. Derely et al., "Raman confocal microscopy and AFM combined studies of cancerous cells treated with Paclitaxel," *Proc. SPIE* **7908**, 79080H (2011).
9. M. Miljković et al., "Label-free imaging of human cells: algorithms for image reconstruction of Raman hyperspectral datasets," *Analyst* **135**(8), 2002–2013 (2010).

10. N. Desai et al., "Increased antitumor activity, intratumor paclitaxel concentrations, and endothelial cell transport of cremophor-free, albumin-bound paclitaxel, ABI-007, compared with cremophor-based paclitaxel," *Clin. Cancer Res.* **12**(4), 1317–1324 (2006).
11. R. M. Gangemi, "Taxol cytotoxicity on human leukemia cell lines is a function of their susceptibility to programmed cell death," *Cancer Chemother. Pharmacol.* **36**(5), 385–392 (1995).
12. A. Gershlick et al., "Inhibition of restenosis with a paclitaxel-eluting, polymer-free coronary stent: the European evaLUation of pacliTaxel Eluting Stent (ELUTES) trial," *Circulation* **109**(4), 487–493 (2004).
13. D. Mastropaolo et al., "Crystal and molecular structure of paclitaxel (taxol)," *Proc. Natl. Acad. Sci. U. S. A.* **92**(15), 6920–6924 (1995).
14. A. K. Singla, A. Garg, and D. Aggarwal, "Paclitaxel and its formulations," *Int. J. Pharmaceut.* **235**(1–2), 179–192 (2002).
15. T. S. R. Devi and S. Gayathri, "FTIR and FT-Raman spectral analysis of paclitaxel drugs," *Int. J. Pharmaceut. Sci. Rev. Res.* **2**(2), 106–110 (2010).
16. M. Argov et al., "Novel steroid carbamates reverse multidrug-resistance in cancer therapy and show linkage among efficacy, loci of drug action and P-glycoprotein's cellular localization," *Eur. J. Pharm. Sci.* **41**(1), 53–59 (2010).
17. J. S. Castro et al., "Heterogeneous and homogeneous nucleation of Taxol crystals in aqueous solutions and gels: effect of tubulin proteins," *Colloids Surf. B Biointerfaces* **76**(1), 199–206 (2010).
18. T. J. Collins et al., "Mitochondria are morphologically and functionally heterogeneous within cells," *Embo. J.* **21**(7), 1616–1627 (2002).
19. S. Y. Jeong and D. W. Seol, "The role of mitochondria in apoptosis," *BMB Rep.* **41**(1), 11–22 (2008).
20. Y. Shi et al., "Titanium dioxide nanoparticles cause apoptosis in BEAS-2B cells through the caspase 8/t-Bid-independent mitochondrial pathway," *Toxicol. Lett.* **196**(1), 21–27 (2010).
21. A. S. Levenson and V. C. Jordan, "MCF-7: the first hormone-responsive breast cancer cell line," *Cancer Res.* **57**(15), 3071–3078 (1997).
22. M. O. Hengartner, "The biochemistry of apoptosis," *Nature* **407**(6805), 770–776 (2000).
23. M. Okada et al., "Label-free Raman observation of cytochrome c dynamics during apoptosis," *Proc. Natl. Acad. Sci. U. S. A.* **109**(1), 28–32 (2012).
24. C. Matthaus et al., "Raman and infrared microspectral imaging of mitotic cells," *Appl. Spectrosc.* **60**(1), 1–8 (2006).
25. M. Kakita, V. Kaliaperumal, and H. O. Hamaguchi, "Resonance Raman quantification of the redox state of cytochromes b and c in-vivo and in-vitro," *J. Biophoton.* **5**(1), 20–24 (2012).
26. K. Brautigam et al., "Raman spectroscopic imaging for the real-time detection of chemical changes associated with docetaxel exposure," *Chemphyschem* **14**(3), 550–553 (2013).